Low concentration amino-bisphosphonates stimulate human keratinocyte proliferation and in vitro wound healing

Filippo Renò, Mario Migliario, Manuela Rizzi, Marco Invernizzi, Carlo Cisari, Mario Cannas

Renò F, Migliario M, Rizzi M, Invernizzi M, Cisari C, Cannas M. Low concentration amino-bisphosphonates stimulate human keratinocyte proliferation and in vitro wound healing. Int Wound J 2012; 9:442–450

ABSTRACT

Amino-bisphosphonates (N-BPs) are widely used to treat a great variety of clinical conditions involving altered calcium metabolism, as well as to prevent bone metastases. The use of N-BPs, however, display well-known side effects, including cellular toxicity, mainly at soft tissue and mucosal level, that arise from N-BPs ability to induce cell apoptosis when administered at clinically relevant concentrations. The aim of this study was to evaluate, in an in vitro wound healing model, the effect of N-BPs low concentration (10 nM–10 μM) stimulation on keratinocyte cellular behaviour. Human keratinocytes were treated with neridronate and zoledronate, two N-BPs with different chemical structure and clinical potency, but sharing a common pharmacological target: farnesyl pyrophosphate (FPP) synthase. Surprisingly, at the tested concentrations, both drugs stimulated keratinocytes proliferation, upregulating cytokeratin 5 while downregulating filaggrin expression, and wound healing ability, without any significant effect on matrix metalloproteinase (MMP)-9 activity. The lack of N-BPs effect on MMP-9 activity indicates that wound closure, in our experimental model, is mainly due to an increase in cell proliferation rather than to an increase in cell migration. Therefore, it can be hypothesised that the observed wound healing results could be ascribed to an N-BPs mediated reduction of FPP endogenous levels, thus suggesting new possible clinical applications for these compounds.

Key words: amino-bisphosphonates • human keratinocytes • wound healing

Authors: F Renò, PhD, Human Anatomy Laboratory, Experimental and Clinical Medicine Department, University of Eastern Piedmont ''A. Avogadro'', Via Solaroli, 17, 28100 Novara, Italy; M Migliario, MD, Dental Clinic, Experimental and Clinical Medicine Department, University of Eastern Piedmont ''A. Avogadro'', Via Solaroli, 17 - 28100 Novara, Italy; M Rizzi, PhD, Human Anatomy Laboratory, Experimental and Clinical Medicine Department, University of Eastern Piedmont ''A. Avogadro'', Via Solaroli, 17, 28100 Novara, Italy; M Invernizzi, PhD, Physical and Rehabilitative Medicine, Azienda Ospedaliera Universitaria 'Maggiore della Carità', via Piazza d'Armi, 1, 28100 Novara, Italy; C Cisari, MD, Physical and Rehabilitative Medicine, Azienda Ospedaliera Universitaria 'Maggiore della Carità', via Piazza d'Armi, 1, 28100 Novara, Italy; M Cannas, MD, Human Anatomy Laboratory, Experimental and Clinical Medicine Department, University of Eastern Piedmont ''A. Avogadro'', Via Solaroli, 17, 28100 Novara, Italy

Address for correspondence: Prof. F Renò, PhD, Experimental and Clinical Medicine Department, University of Eastern Piedmont ''A. Avogadro'', Via Solaroli 17, 28100 Novara, Italy

E-mail: filippo.reno@med.unipmn.it

international wound journal

INTRODUCTION

Bisphosphonates (BPs) are synthetic compounds used in the clinical practice since the end of the 1960s for the treatment of various diseases of bone, tooth and calcium metabolism thanks to their high affinity for bone and anti-resorptive activity (1–3). In particular, starting from 1970s, these compounds entered in the oncological clinical practice for the treatment and prevention of skeletal complications of multiple myeloma or bone metastases arising from different types of cancer (4).

The chemical structure of BPs is characterised by the presence of a P-C-P structure allowing them to bind divalent ions, such as Ca^{++} (4,5). The P-C-P structure can undergo a great number of modifications, by changing the two lateral chains on the carbon atom (conventionally identified as R1 and R2), resulting in extensive alterations in their physicochemical, biological, therapeutic and toxicological characteristics (1,2). In particular, R1 substituents modulate BPs Ca^{++} chelating ability, while R2 substituents are mainly involved in mediating their anti-resorptive effects. The presence of nitrogen substituents at critical positions in R2 side chain is essential in determining drug potency, as nitrogen-containing BPs are up to 100-fold more potent than non amino-containing compounds. (4,6). Moreover, BPs' high chemical stability accounts for the inability of the human body to metabolise them, finally resulting in their rapid clearance from the circulation (half-life in the range of hours) and unaltered excretion (4,5,7).

BPs mechanisms of action are complex, and their relative potency varies between the different compounds, according to the R1 and R2 side chain nature. On the basis of their mechanism of action, BPs can be classified into two distinct groups: non nitrogen-containing compounds (non N-BPs), most closely resembling inorganic pyrophosphate (PPi), and nitrogen-containing compounds (N-BPs), that interfere with protein prenylation and finally affect the intracellular trafficking of regulatory proteins. In particular, non N-BPs are incorporated into ATP containing compounds, forming non hydrolysable toxic analogues, thus resulting in energy starvation and consequent cell death (6–9). On the other hand, N-BPs inhibit the farnesyl pyrophosphate (FPP) synthase, leading to a decrease in the formation of isoprenoid lipids and finally to a reduction in protein prenylation, a post-translational covalent modification playing a key role in the intracellular trafficking of regulatory proteins, resulting in cellular microarchitecture loss and osteoclast apoptosis. N-BPs mechanism of action determines a slower rate of bone turnover and an altered bone remodelling. Interestingly, whereas FPP synthase is ubiquitous in mammalian cells, N-BPs seem to induce apoptosis in osteoclasts as a direct consequence of their strong affinity for bone matrix and their local accumulation (6–9).

In addition to their well-known anti-resorptive effects, BPs have also been shown to have anti-angiogenic, anti-proliferative and immunological activities (10) along with anti-cancer activities as suggested also by direct BPs apoptotic effects on different tumour cell lines (3,11,12).

Therapy with BPs shows well-known side effects, classified into four main groups: acute phase reactions, gastrointestinal effects, renal side effects and BPs-associated osteonecrosis of the jaws (ONJ) (13).

Although BPs main target is bone and they are only briefly present in serum, their toxicity towards soft tissues, resulting in gastric erosion and both oral and gastric mucosa ulcers, is a well-known and documented side effect associated with oral administration of N-BPs.

The mechanism underlying N-BPs-induced gastric damage is not clearly understood, even if experimental observations indicate that BPs exert gastric damage by acting as topical irritants on the gastric mucosa. In vivo studies with rats showed that BPs-induced gastrointestinal irritation is not due to their ability to chelate divalent ions such as Ca^{++}, and also that the presence of acid in the stomach is not a predominant mechanism of BP-induced damage (14). Lichtenberger *et al*. hypothesised that BPs might cause topical injury of the upper gastrointestinal tract mucosa by attenuating the tissues hydrophobic barrier to luminal acid (15). As BPs anti-resorptive potency is related to the nature of the side chain attached to the germinal carbon of the P-C-P backbone, a similar rank order potency has been described for gastrointestinal effects, suggesting that these side effects could be mechanism based. Moreover, the conclusion that the observed gastrointestinal injury might be due to topical irritation is supported by the clinical observation that such damages are uncommon

Key Points

- bisphosphonates (BPs) are widely used drugs for the treatment of osteoporosis and bone metastases.
- BPs activity depends on R1 and R2 side chains substituents.
- nitrogen substituents in R2 increase drug anti-resorptive activity.
- nitrogen-containing BPs (N-BPs) inhibit farnesyl pyrophosphate (FPP) synthase and intracellular protein traffic.
- BPs side effects towards soft tissues have been reported.
- N-BPs strongly reduce oral keratinocytes proliferation and migration.
- in this study low concentrations of N-BPs have been used in an in vitro wound healing model.
- low doses of N-BPs increase human keratinocytes proliferation.
- low doses of N-BPs stimulate in vitro wound healing.
- the observed effects could be related to a direct effect on the FPP production.

in patients undergoing intravenous BPs administration (16–18).

It has been hypothesised that BPs treatment-induced an early apoptosis of oral keratinocytes, resulting in a damage of the mouth immune barrier and subsequent bacterial secondary colonisation of the injured tissue. This condition might involve a local decrease in pH values, allowing an increased BPs release from bones finally resulting in oral epithelium toxicity (7).

BPs cytotoxic effect on epithelial cells of different origin, such as that from the oral mucosa, has not been investigated in detail yet (16) even if Pabst *et al*. (13) observed that in a commercial human oral keratinocyte (HOK) cell line, N-BPs strongly reduced cell viability and induce cell apoptosis starting from a drug concentration of 50 μmol/l.

The aim of this study was to evaluate the effects of low concentrations (10 nM–10 μM) of two different N-BPs [neridronate (Ner) and zoledronate (Zol), Figure 1] on human keratinocytes proliferation and migration in an in vitro wound healing model.

MATERIALS AND METHODS

Cell culture

Spontaneously immortalised keratinocytes (HaCaT), isolated from human adult skin (19), were a kind gift of Dr M De Andrea from the Microbiology Laboratory, University of Eastern Piedmont ''A. Avogadro''. Cells were grown in culture flask (75 cm^2) in Dulbecco's modified Eagle's medium (DMEM) medium (Euroclone, Milan, Italy) supplemented with 10% heat inactivated foetal bovine serum (FBS) (Euroclone, Milan, Italy), penicillin (100 U/ml), streptomycin (100 mg/ml) and L-glutamine (2 mM) (Euroclone, Milan, Italy) in a humidified atmosphere containing 5% CO_2 at 37°C.

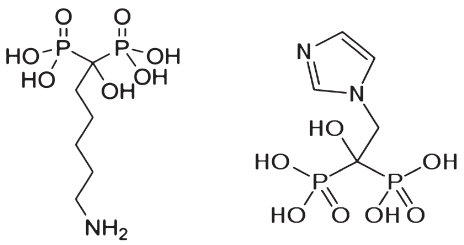

Figure 1. Schematic structure of the two tested N-BPs, neridronate (Ner) and zoledronate (Zol).

Bisphosphonate treatment

HaCaT cells were treated with commercial bisphosphonate solutions for clinical use [Aclasta (Novartis Pharma GmbH, Nürnberg, Germany) for zoledronic acid (Zol) and Nerixia (Abiogen Pharma S.p.A., Ospedaletto, Italy) for neridronic acid (Ner)]. All the aqueous solutions for intravenous administration were diluted to the tested concentrations (10 nM–10 μM) in DMEM without FBS just before cell treatments. Control samples (Cnt) were left untreated and incubated in complete DMEM medium. For all the experiments, cells were incubated with the BPs of interest for 48 hours (HaCaT duplication time).

Cell proliferation

Aliquots of 5×10^4 cells were seeded in cell culture multi-wells and allowed to adhere overnight. Inadherent cells were removed by gentle wash with phosphate buffer solution (PBS, pH = 7·4), and drugs were added in fresh medium, while fresh medium without drugs was added to Cnt. After 48 hours of incubation, cell proliferation was quantified using both a fluorimetric method based on the quantification of resazurin reduction by viable cells (Tox-8, Sigma Aldrich, Milwaukee, WI) and cell counting. Briefly, 25 μl of dye was dissolved in 0·5 ml of complete cell growth medium, and after 4 hours the optical density was measured at 620 nm. Cell proliferation was expressed as optical density (OD) variation ± standard deviation (SD). At the end of the experiment, both control and treated samples were fixed using 3·7% formaldehyde, 3% sucrose solution in PBS at 4°C and then stained with a 1% toluidine blue solution. Stained samples were observed using a reverse optical microscope (Leica DMIL, Leica Microsystems Wetzlar GmbH, Wetzlar, Germany) to evaluate cell density. Cells were counted, and results were expressed as cells/mm^2 ± SD.

Reverse transcriptase polymerase chain reaction

Total cellular RNA was extracted after 48 hours treatment using Qiagen RNeasy MiniKit (Qiagen, Hilden, Germany) following manufacturer's protocol. Complementary DNA (cDNA) were prepared from total RNA using the ImProm-II Reverse Transcription System (Promega, Madison, WI) and 0·5 μg oligo$(dT)_{15}$

primers in a final volume of 20 µl. Briefly, the RNA-primers mixture was heated at 70°C for 5 minutes and then $MgCl_2$, reaction buffer, dNTPs mix, ribonuclease inhibitor and reverse transcriptase (RT) enzyme were added according to the manufacturer's protocol. The reaction mixture was equilibrated at 25°C for 5 minutes and then incubated at 42°C for 1 hour. RT was finally thermally inactivated by incubation at 70°C for 15 minutes. The resulting cDNA was amplified by polymerase chain reaction (PCR) using synthetic oligonucleotide primers specific for human Filaggrin (Fil), cytokeratin 5 (K5) and β-actin, designed using the primer-blast tool software from NCBI. Forward and reverse primer sequences and the expected size of PCR products are indicated in Table 1. Reaction products were separated onto 1·8% Tris-borate-EDTA (TBE)-agarose gel and stained with ethidium bromide. DNA molecular weight marker (Sigma Aldrich, Milwaukee, WI) was used as a size marker. Stained gels were acquired in digital format, and gene expression has been evaluated by means of densitometric analysis using ImageJ software.

In vitro scratch assay

Cell migration has been evaluated by in vitro scratch assay (20). HaCaT cells were seeded in 0·38 cm^2 culture wells and grown in complete DMEM medium to reach a confluent monolayer. Cell monolayers were then mechanically scratched with a yellow tip (diameter = 2 mm), and cell debris were removed by gentle wash with fresh medium. Some Cnt were immediately fixed using 3·7% formaldehyde, 3% sucrose solution in PBS to fix the initial scratch width, while the other samples were treated with BPs or left untreated and incubated at 37°C in a humidified atmosphere containing 5% CO_2 for 48 hours.

At the end of the experiment, both control and treated samples were fixed using 3·7% formaldehyde, 3% sucrose solution in PBS at 4°C and then stained with a 1% toluidine blue solution. Stained samples were then observed using a reverse optical microscope (Leica DMIL, Leica Microsystems Wetzlar GmbH, Wetzlar, Germany) to evaluate wound closure. In vitro wound healing response was evaluated by determining the percentage of wound closure, considering the values referred to time zero as 0%. Wound width has been measured using Leica QWin software (Leica Microsystems Imaging Solutions Ltd, Cambridge, UK), and wound closure has been expressed as mean ± SD values.

Gelatine zymography

To detect matrix metalloproteinases (MMP)-2 and MMP-9 activities, conditioned media from HaCaT grown for 48 hours in presence or absence of drugs were separated by electrophoresis on sodium dodecyl sulphate (SDS)-polyacrylamide gels containing 0·2% gelatine. Samples were loaded onto zymograms without denaturation. After running, gels were washed at room temperature for 2 hours in 2·5% Triton X-100 solution and incubated overnight at 37°C in 0·5 M Tris–HCl, 0·2 M NaCl, 5 mM $CaCl_2$, 1 mM $ZnCl_2$ buffer. Gels were then fixed in MeOH/acetic acid (50:10) solution and stained in 0·5% Coomassie Blue in MeOH/acetic acid (40:10) solution. Images of stained gels were acquired after appropriate destaining. Gelatinolytic activity was detected as white bands on a dark blue background and quantified by densitometric analysis using ImageJ software.

Statistical analysis

Unpaired Student's *t*-tests were performed for statistical analysis. Probability values of $P < 0·05$ were considered statistically significant. Data were expressed as mean ± SD values.

Table 1 Primer sequences used for reverse transcriptase polymerase chain reaction (RT-PCR) analysis and expected size of the resulting RT-PCR amplification products

Gene	Primers	Product size (bp)
K5	Forward 5′-CAC CAA GAC TGT GAG GCA GA-3′ Reverse 5′-CAT CCA TCA GTG CAT CAA CC-3′	274
Filaggrin	Forward 5′-TGA TGC AGT CTC CCT CTG TG-3′ Reverse 5′-TGT TTC TCT TGG GCT CTT GG-3′	338
β-actin	Forward 5′-ACA CTG TGC CCA TCT ACG AGG GG-3′ Reverse 5′-ATG ATG GAG TTG AAG GTA GTT TCG TGG AT-3′	360

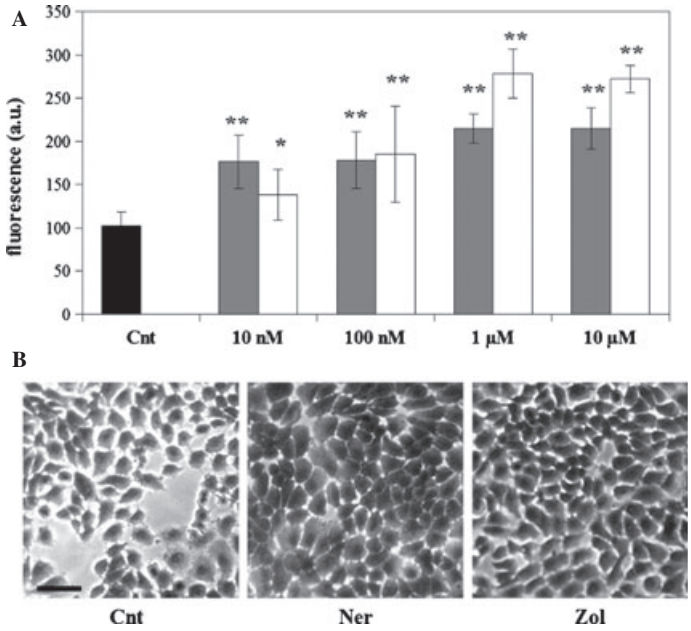

Figure 2. (A) Determination of HaCaT cells proliferation by means of commercial Tox-8 assay. Fluorescence values are expressed as arbitrary units (a.u.) ± SD. Black bars = control, grey bars = neridronate, white bars = zoledronate. $*P < 0{\cdot}05$ and $**P < 0{\cdot}001$ compared with control samples. (B) Optical microscopy images of control and N-BPs (Neridronate and Zoledronate)-treated cells after 48 hours of incubation, stained with toluidine blue. Magnification = 10×. Scale bar = 30 µm.

RESULTS

Cell proliferation

The effects of the N-BPs Zol and Ner on cell proliferation were analysed by measuring the increase of fluorescence values due to the bioreduction of resazurine dye by viable cells using the commercial Tox-8 assay. As shown in Figure 2A both drugs, after 48 hours of incubation, induced a significant dose-dependent increase in cell proliferation compared with control conditions. Zoledronic acid showed the strongest effect on cell proliferation even if both N-BPs reached a maximum effect at 1 µM concentration. The biochemical evidence of increased cell proliferation was confirmed by morphological analysis (Figure 2B). In fact, in Cnt, cellular density after 48 hours of incubation was 1611 ± 122 cells/mm^2, while in samples treated with both 10 µM Ner and Zol, the cellular concentration was 1892 ± 111 cells/mm^2 and 2042 ± 296 cells/mm^2, respectively ($P < 0{\cdot}05$).

Proliferation and differentiation markers expression in cells grown in the presence of N-BPs

Total RNA was extracted from keratinocytes grown for 48 hours in control and N-BPs containing medium. RNA was reverse-transcribed and amplified by PCR to assess K5, a keratinocyte specific proliferation marker (21), and Fil, a keratinocyte differentiation marker (21), gene expression. β-actin was used as housekeeping gene.

As shown in Figure 3A, B, Ner was strongly able to increase K5 expression starting from the lower concentration used (10 nM), while reducing the differentiation marker Fil expression that became almost undetectable at 10 µM concentration (Figure 3B). Similar effects were observed stimulating HaCaT cells with Zol (Figure 4A, B). In fact, Zol increased the expression of the proliferation marker K5 in a dose-dependent fashion, decreasing, at the same time, Fil expression.

In vitro wound healing

The effects of Zol and Ner on wound healing ability of HaCaT cells were studied using the scratch assay. As shown in Figure 5A, both the N-BPs Zol and Ner strongly induced a dose-dependent wound closure. In particular, Ner seems to act at lower concentrations compared to Zol. In fact, while the percentage of wound closure measured in Cnt after 48 hours was $60 \pm 6\%$, 10 nM Ner was able to increase the percentage of wound closure to $81 \pm 12\%$ ($P < 0{\cdot}05$). Instead Zol, used at the

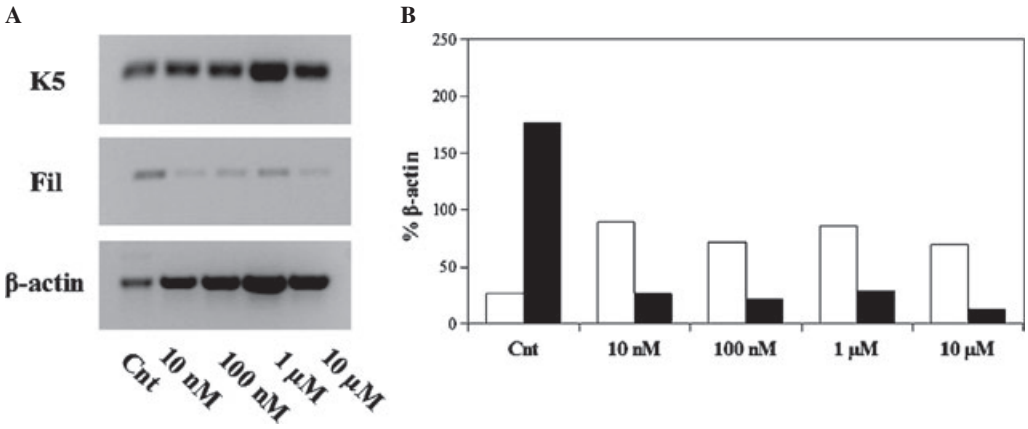

Figure 3. (A) Representative 1·8% agarose-TBE gels, stained with ethidium bromide, showing polymerase chain reaction (PCR) amplification products for cytokeratin 5 (K5), filaggrin (Fil) and β-actin in both control and neridronate-treated cells. (B) Densitometric quantification of K5 and Fil gene expression, normalised on the expression of the housekeeping gene β-actin. Black bars = Fil, white bars = K5.

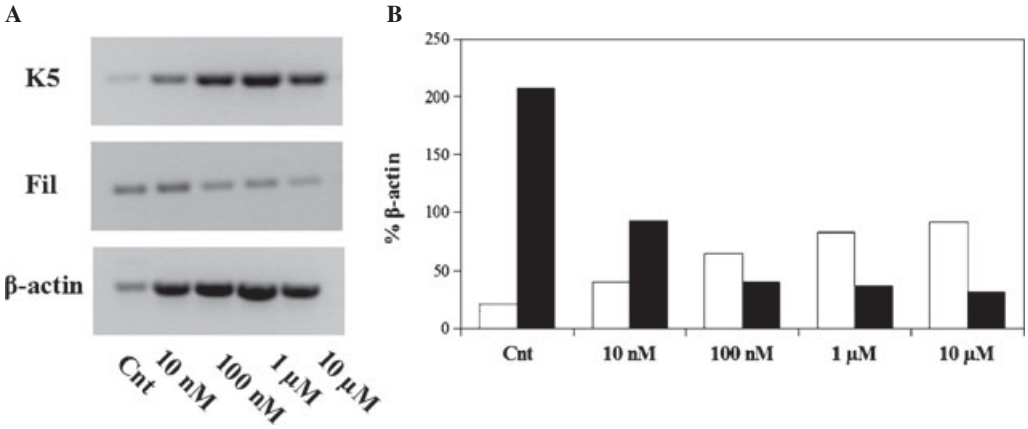

Figure 4. (A) Representative 1·8% agarose-TBE gel, stained with ethidium bromide, showing polymerase chain reaction amplification products for cytokeratin 5 (K5), filaggrin (Fil) and β-actin in both control and zoledronate-treated cells. (B) Densitometric quantification of K5 and Fil gene expression, normalised on the expression of the housekeeping gene β-actin. Black bars = Fil, white bars = K5.

same concentration, had no effects on control in vitro wound closure (Figure 5B). On the other hand, starting from 100 nM concentration, there were no differences in the effects of the two drugs on keratinocytes wound healing ability.

MMPs activity

To evaluate the ability of N-BPs to induce cell migration along with cell proliferation in HaCaT cells, the presence and activity of MMP-2 and MMP-9 involved in keratinocytes migration were measured by gelatine zymography in the conditioned medium obtained by scratch assay samples. As shown in the representative zymograms in Figure 6, both Ner (A) and Zol (B) were unable to modulate both MMP-2 (mostly derived from FBS, data not shown) and MMP-9 expression. Therefore, the wound closure effect observed was probably due mostly to HaCaT proliferation.

DISCUSSION

N-BPs drugs are clinically used for the treatment of various bone, tooth and calcium metabolism diseases, as well as for the prevention of skeletal metastases arising from different types of cancer (4). These pharmacological treatments have a wide range of known side effects, including mucosal toxicity, especially at oral and gastrointestinal levels when orally

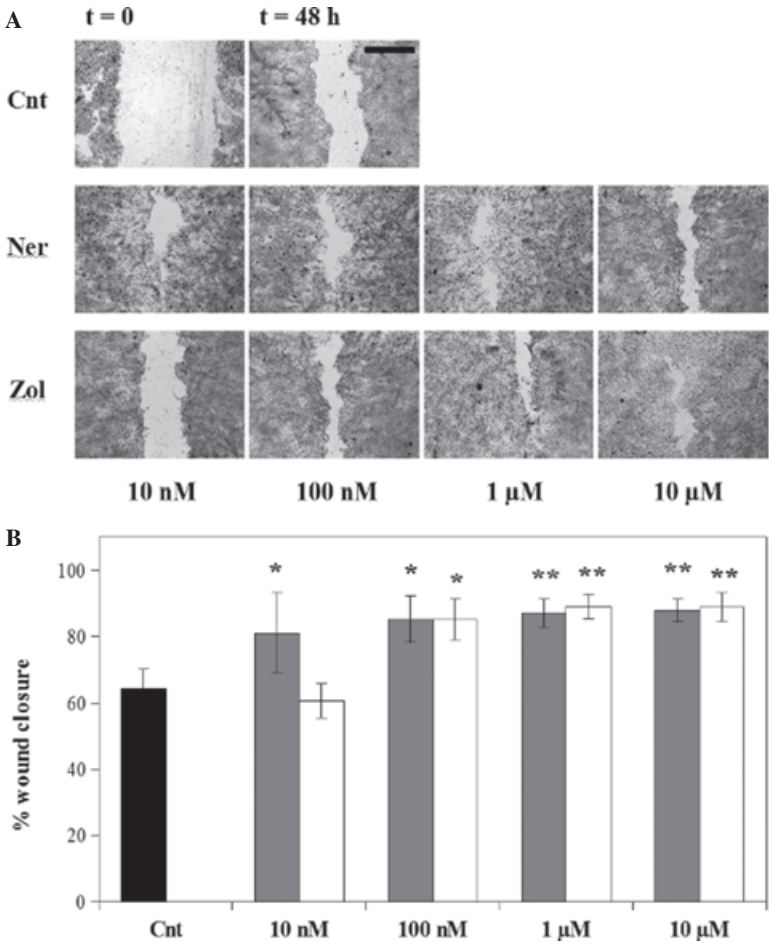

Figure 5. (A) Representative optical microscopy images of in vitro wound healing (scratch) assay. Fixed cells were stained with toluidine blue solution. Magnification = 4×. Scale bar = 1 mm. (B) Quantification of wound closure. Results are expressed as % of wound closure, setting time zero = 0%. Black bars = control, grey bars = neridronate, white bars = zoledronate. $*P < 0{\cdot}05$ and $**P < 0{\cdot}001$ compared with control samples.

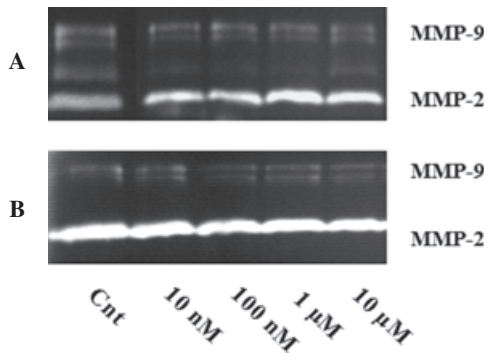

Figure 6. Representative zymography of cell growth medium from 48 hours control (Cnt) and Ner (A) and Zol (B) treated cells.

administered. In fact, the most used N-BPs are now administered by venous infusion to avoid high local concentration of the drug. Nevertheless, it has been reported that even after intravenous infusion, gastric ulcerations could take place (7).

The observed cell toxicity mainly arise from N-BPs-induced apoptosis, in fact, it has been reported by different authors that these compounds exert pro-apoptotic effects onto mouse keratinocytes and gastrointestinal cells (16,17), as well as pre-endothelial and endothelial cells (22,23). Moreover, in HOKs, it has been shown that 50 μmol/l of Zol decreased cell proliferation and migration and increased apoptosis (13), while pamidronate, another N-BP with shorter linear R2 side chain compared with Ner, inhibited mouse oral keratinocytes proliferation and wound healing at 100 μM concentration (16). Interestingly, lower concentrations of pamidronate had no negative effects on cells proliferation and after 7 days of

incubation seemed to even stimulate cell proliferation (16). This paradoxical effect was not explained by the authors.

In this study, we tested the effects of low concentrations (10 nM–10 μM) of two N-BPs (the linear N-BP Ner and the heterocyclic N-BP Zol, known to be one of the most potent N-BP today commercially available, because of the presence of the nitrogen atom in the heterocyclic ring) on human spontaneously immortalised keratinocytes (HaCaT, period of duplication of about 48 hours).

Surprisingly, in our experimental model, the two N-BPs were able to induce dose-dependent cell proliferation, stimulate K5 gene expression and increase keratinocytes in vitro wound closure ability without affecting the expression of MMP-9, one of the MMPs involved in keratinocytes migration. To our knowledge, these experimental data are in contrast with all the existing studies dealing with the effects of BPs on keratinocytes cellular behaviour, but, so far, no experimental protocol used this low range of BPs concentrations. A possible explanation of the observed phenomena could be related to an interesting mechanism of wound healing inhibition recently described (24). It has been reported that FPP, the product of the FPP synthase, the main target of N-BPs pharmacological action, is able to inhibit epithelization and wound healing by acting as a glucocorticoid receptor (GR) agonist (24).

FPP binding to GR, in fact, inhibits human epidermal keratinocytes migration, and this inhibition has been shown to be reverted by the addition of mevastatine, a statine that reduces FPP endogenous levels without affecting cholesterol synthesis or protein farnesylation (24).

Our data could suggest that low concentrations of BPs mainly affect FPP levels stimulating wound healing, just as observed for mevastatine addition to HEK cells in absence of any other drug (24). It is noteworthy that Zol IC_{50} for FPP synthase is 475 ± 10 nM (25), a concentration that is in the range of N-BPs concentrations able to stimulate keratinocytes proliferation.

Even if these data are extremely preliminary and further work needs to be performed to better elucidate the cellular mechanisms involved in the observed phenomena, they can suggest new clinical applications for BPs in a very promising field such as cutaneous wound healing.

REFERENCES

1 Fleisch H. Bisphosphonates: mechanisms of action. Endocr Rev 1998;19:80–100.
2 Fleisch H. Development of bisphosphonates. Breast Cancer Res 2002;4:30–4.
3 Guise TA. Antitumor effects of bisphosphonates: promising preclinical evidence. Cancer Treat Rev 2008;34:S19–24.
4 Russell RGG, Watts NB, Ebetino FH, Rogers MJ. Mechanisms of action of bisphosphonates: similarities and differences and their potential influence on clinical efficacy. Osteoporos Int 2008;19:733–59.
5 Roelofs AJ, Thompson K, Gordon S, Rogers MJ. Molecular mechanisms of action of bisphosphonates: current status. Clin Cancer Res 2006;12(20 Suppl):6222s–30s.
6 Rogers MJ, Watts DJ, Russell RGG. Overview of bisphosphonates. Cancer 1997;80(8 Suppl):1652–60.
7 Magremanne M. Ostéochimionécrose maxillo-mandibulaire. [Osteoporosis, bisphosphonates and jaws osteochemonecrosis]. Rev Med Brux 2008;29:262–6.
8 Hasmim M, Bieler G, Rüegg C. Zoledronate inhibits endothelial cell adhesion, migration and survival through the suppression of multiple, prenylation-dependent signaling pathways. J Thromb Haemost 2007;5:166–73.
9 Drake MT, Clarke BL, Khosla S. Bisphosphonates: mechanism of action and role in clinical practice. Mayo Clin Proc 2008;83:1032–45.
10 Facon T, Bensadoun RJ, Blanc JL, Confavreux C, Gourmet R, Maes JM, Penel G, Vieillard MH, Woeller A. Ostéonécrose des maxillaires et bisphosphonates en cancérologie. [Osteonecrosis of the jaw and bisphophonates in oncology]. Bull Cancer 2008;95:413–8.
11 Green JR, Guenther A. The backbone of progress – preclinical studies and innovations with zoledronic acid. Crit Rev Oncol Hematol 2011; 77(1 Suppl): S3–12.
12 Coleman R. The use of bisphosphonates in cancer treatment. Ann NY Acad Sci 2011;1218:3–14.
13 Pabst AP, Ziebart T, Koch FP, Taylor KY, Al-Nawas B, Walter C. The influence of bisphosphonates on viability, migration, and apoptosis of human oral keratinocytes – in vitro study. Clin Oral Invest. In press.
14 Blank MA, Ems BL, Gibson GW, Myers WR, Berman SK, Philips RJ, Smith PN. Nonclinical model for assessing gastric effects of bisphosphonates. Dig Dis Sci 1997;42:281–8.
15 Lichtenberger LM, Romero JJ, Gibson GW, Blank MA. Effect of bisphosphonates on surface hydrophobicity and phosphatidylcholine concentration of rodent gastric mucosa. Dig Dis Sci 2000;45:1792–801.
16 Landesberg R, Cozin M, Cremers S, Woo V, Kousteni S, Sinha S, Garret-Sinha LA, Raghavan S. Inhibition of oral mucosal cell wound

healing by bisphosphoonates. J Oral Maxillofac Surg 2008;66:839–47.
17 Reszka AA, Halasy-Nagy J, Rodan GA. Nitrogen-bisphosphonates block retinoblastoma phosphorylation and cell growth by inhibiting the cholesterol biosynthetic pathway in a keratinocyte model for esophageal irritation. Mol Pharmacol 2001;59:193–202.
18 Wallace JL, Dicay M, McKnight W, Bastaki S, Blank MA. N-bisphosphonates cause gastric epithelial injury independent of effects on the microcirculation. Aliment Pharmacol Ther 1999;13:1675–82.
19 Boukamp P, Petrussevska RT, Breitkreutz D, Hornung J, Markham A, Fusenig NE. Normal keratinization in a spontaneously immortalized aneuploid human keratinocyte cell line. J Cell Biol 1988;106:761–71.
20 Liang CC, Park AY, Guan JL. In vitro scratch assay: a convenient and inexpensive method for analysis of cell migration in vitro. Nat Protoc 2007;2:329–33.
21 Presland RB, Dale BA. Epithelial structural proteins of the skin and oral cavity: function in health and disease. Crit Rev Oral Biol Med 2000;11: 383–408.
22 Walter C, Pabst A, Ziebart T, Klein MO, Al-Nawas B. Bisphosphonates affect migration ability and cell viability of HUVEC, fibroblasts and osteoblasts in vitro. Oral Diseases 2011;17:194–99.
23 Bezzi M, Hasmim M, Bieler G, Dormond O, Rüegg C. Zoledronate sensitizes endothelial cells to tumor necrosis factor-induced programmed cell death: evidence for the suppression of sustained activation of focal adhesion kinase and protein kinase B/Akt. J Biol Chem 2003;278:43603–14.
24 Vukelic S, Stojadinovic O, Pastar I, Vouthounis C, Krzyzanowska A, Das S, Samuels HH, Tomic-Canic M. Farnesyl pyrophosphate inhibits epithelialization and wound healing through the glucocorticoid receptor. J Biol Chem 2010;285:1980–8.
25 Kavanagh KL, Guo K, Dunford JE, Wu x, Knapp S, Ebetino FH, Rogers MJ, Russell RGG, Oppermann U. The molecular mechanism of nitrogen-containing bisphosphonates as antiosteoporosis drugs. PNAS 2006;103:7829–34.